

Electronic Supplementary Information

Design of robust rod-packing scandium-organic framework for C₂Hx/CO₂ separation, CO₂ storage and catalytic CO₂ cycloaddition

Hong-Juan Lv, Shu-Cong Fan, Yu-Cheng Jiang, Shu-Ni Li, and Quan-Guo Zhai**

Key Laboratory of Macromolecular Science of Shaanxi Province, Key Laboratory of Applied Surface and Colloid Chemistry, Ministry of Education, School of Chemistry & Chemical Engineering, Shaanxi Normal University, Xi'an, Shaanxi, 710062, China.

*Corresponding authors

E-mail: jyc@snnu.edu.cn (Y.-C. Jiang); zhaiqg@snnu.edu.cn (Q.-G. Zhai)

1. Isosteric Analysis of the Heat of Adsorption

To extract the coverage-dependent isosteric heat of adsorption, the data were modeled with a virial-type expression composed of parameters a_i and b_i that are independent of temperature^[S1]:

$$\ln P = \ln N + \frac{1}{T} \sum_{i=0}^m a_i N^i + \sum_{i=0}^n b_i N^i \quad (\text{S1})$$

$$Q_{st} = -R \sum_{i=0}^m a_i N^i \quad (\text{S2})$$

where P is pressure, N is the amount adsorbed (or uptake), T is temperature, and m and n determine the number of terms required to adequately describe the isotherm.

2. Calculations of Ideal Adsorbed Solution Theory (IAST)

To perform the integrations required by Ideal Adsorbed Solution Theory (IAST), the single-component isotherms should be fitted by a proper model, and the Langmuir-Freundlich (LF) equation were found to the best fit to the experimental data^[S2]:

$$q = q_m * \frac{b * p^{1/n}}{1 + b * p^{1/n}} \quad (\text{S3})$$

where p is the pressure of the bulk gas at equilibrium with the adsorbed phase (kPa), q is the adsorbed amount per mass of adsorbent (mmol g⁻¹), q_m is the saturation capacities of site (mmol g⁻¹), b is the affinity coefficients of site (1/kPa), and n represent the deviations from an ideal homogeneous surface. The adsorption selectivity is defined by

$$S_{A/B} = \frac{x_A/y_A}{x_B/y_B} \quad (\text{S4})$$

where x_i and y_i are the mole fractions of component i ($i = A$ and B) in the adsorbed and bulk phases, respectively. Note that in the Henry regime $S_{A/B}$ is identical to the ratio of the Henry constants of the two species.

3. Breakthrough Experiments

The actual CO₂ capture amount and separation factor of binary mixture for C₂H₄/CO₂, C₂H₂/CO₂, C₂H₆/CO₂ were calculated by reported method^[S3]. The actual adsorbed amount of gas i (q_i) is calculated from the breakthrough curve by the equation:

$$q_i = \frac{F_i * t_0 - V_{dead} - \int_0^{t_0} F_e \Delta t}{m} \quad (\text{S5})$$

The separation factor (α) of the breakthrough experiment is determined as

$$\alpha = \frac{q_1 * y_2}{q_2 * y_1} \quad (\text{S6})$$

where F_i is the influent flow rate of the specific gas (ml min⁻¹); t_0 is the adsorption time (min); V_{dead} is the dead volume of the system (cm³); F_e is the effluent flow rate of the

specific gas (ml min^{-1}); and m is the mass of the sorbent (g). y_i is the molar fraction of gas i in the gas mixture.



Fig. S1 The photo of optical microscope for SNNU-616-Sc.

Table S1 The crystal data and structure refinements for SNNU-616-Sc

Compound	SNNU-616-Sc
CCDC Number	2242282
Empirical formula	$\text{C}_{144}\text{H}_{99}\text{N}_6\text{O}_{54}\text{Sc}_9$
Formula weight	3019.66
Temperature (K)	170.01
Crystal system	Trigonal
Space group	$R\bar{3}$
$a(\text{\AA})$	42.606(3)
$b(\text{\AA})$	42.606(3)
$c(\text{\AA})$	26.6987(16)
α (deg)	90
β (deg)	90
γ (deg)	120
Volume (\AA^3)	41973(7)
Z	6
ρ_{calc} g/cm ³	0.755
μ/mm^{-1}	1.458
$F(000)$	9756.0
Crystal size/mm ³	0.15 × 0.12 × 0.08
Radiation	GaK α ($\lambda = 1.34139$)
2 Θ range for data collection/°	6.126 to 110.746
Index ranges	-50 ≤ h ≤ 52, -52 ≤ k ≤ 51, -16 ≤ l ≤ 32
Reflections collected	153911
R_{int}	0.1352
Data/restraints/parameters	15898/469/646
Goodness-of-fit on F^2	0.798
$R_1^{\text{a}}, wR_2^{\text{b}}$ [$I > 2\sigma(I)$]	0.0856, 0.2484
$R_1^{\text{a}}, wR_2^{\text{b}}$ (all data)	0.1301, 0.2652

$$^a R_1 = \Sigma |F_o| - |F_c| / \Sigma |F_o|. \quad ^b wR_2 = [\Sigma w(F_o^2 - F_c^2)^2 / \Sigma w(F_o^2)^2]^{1/2}$$

Table S2 The selected bond angles ($^{\circ}$) for SNNU-616-Sc

SNNU-616-Sc

Sc1-O3 ¹	2.046(4)	Sc3-O11	2.049(4)
Sc1-O5 ³	2.062(3)	Sc3-O2 ⁵	2.065(3)
Sc1-O5	2.063(3)	Sc3-O10 ⁷	2.063(3)
Sc1-O7	2.061(3)	Sc4-O12	2.058(4)
Sc2-O4 ¹	2.060(3)	Sc4-O9 ⁷	2.099(5)
Sc2O8	2.066(4)	Sc4-O1 ⁵	2.080(4)
Sc2-O6	2.033(5)	Sc4-O13	2.107(5)
Sc2-O16 ⁶	2.114(5)	Sc4-O18	2.010(6)
Sc2-O17 ⁶	2.043(6)	Sc4-O15	2.133(5)
Sc2-O14 ⁶	2.113(4)		

¹2/3-Y,1/3+X-Y,1/3+Z; ²-1/3+Y,1/3-X+Y,4/3-Z; ³1/3-X,2/3-Y,5/3-Z; ⁴1/3-X,2/3-Y,2/3-Z; ⁵2/3-Y,1/3+X-Y,-2/3+Z; ⁶+Y,-X+Y,1-Z; ⁷1/3-Y,2/3+X-Y,-1/3+Z; ⁸1/3+Y-X,2/3-X,-1/3+Z; ⁹1/3+Y-X,2/3-X,2/3+Z; ¹⁰-1/3+Y-X,1/3-X,1/3+Z; ¹¹-Y+X,+X,1-Z

Table S3 The selected bond angles for SNNU-616-Sc

SNNU-616-Sc

O3 ¹ -Sc1-O3 ²	180.0	O12-Sc4-O9 ⁷	90.05(15)
O3 ¹ -Sc1-O5 ³	87.64(15)	O12-Sc4-O1 ⁵	93.53(15)
O3 ² -Sc1-O5 ³	92.35(15)	O12-Sc4-O13	84.28(17)
O3 ² -Sc1-O5	87.66(15)	O12-Sc4-O15	178.2(2)
O3 ¹ -Sc1-O7	91.81(14)	O9 ⁷ -Sc4-O13	84.79(18)
O3 ² -Sc1-O7	88.20(14)	O9 ⁷ -Sc4-O15	88.1(2)
O3 ² -Sc1-O7 ³	91.80(14)	O1 ⁵ -Sc4-O9 ⁷	92.55(17)
O3 ¹ -Sc1-O7 ³	88.19(14)	O1 ⁵ -Sc4-O13	176.54(17)
O5-Sc1-O5 ³	180.0	O1 ⁵ -Sc4-O15	86.61(18)
O7 ³ -Sc1-O5	86.73(14)	O13-Sc4-O15	95.5(2)
O7 ³ -Sc1-O5 ³	93.27(14)	O18-Sc4-O12	87.98(19)
O7-Sc1-O5	93.26(14)	O18-Sc4-O9 ⁷	177.28(17)
O7-Sc1-O7 ³	180.0	O18-Sc4-O1 ⁵	85.69(19)
O11 ⁴ -Sc3-O11	180.0	O18-Sc4-O13	96.88(19)
O11-Sc3-O2 ⁵	90.35(15)	O18-Sc4-O15	93.8(2)
O11-Sc3-O2 ²	89.65(15)	O4 ¹ -Sc2-O8	94.48(15)
O11-Sc3-O10 ⁶	86.75(15)	O4 ¹ -Sc2-O16 ⁶	85.84(17)
O11 ⁴ -Sc3-O10 ⁶	93.25(15)	O4 ¹ -Sc2-O14 ⁶	178.23(17)
O11 ⁴ -Sc3-O10 ⁷	86.75(15)	O8-Sc2-O16 ⁶	176.80(19)

O2 ⁵ -Sc3-O2 ²	180.0	O8-Sc2-O14 ⁶	83.75(18)
O10 ⁶ -Sc3-O2 ²	94.09(14)	O6-Sc2-O4 ¹	90.76(16)
O10 ⁷ -Sc3-O2 ⁵	94.08(14)	O6-Sc2-O8	92.87(17)
O10 ⁶ -Sc3-O2 ⁵	85.92(14)	O6-Sc2-O16 ⁶	83.94(18)
O10 ⁷ -Sc3-O2 ²	85.91(14)	O6-Sc2-O14 ⁶	89.3(2)
O10 ⁶ -Sc3-O10 ⁷	180.00(15)	O6-Sc2-O17 ⁶	178.00(18)
O17 ⁶ -Sc2-O8	85.14(18)	O14 ⁶ -Sc2-O16 ⁶	95.9(2)
O17 ⁶ -Sc2-O16 ⁶	98.04(19)	O17 ⁶ -Sc2-O4 ¹	89.13(17)
O17 ⁶ -Sc2-O14 ⁶	90.7(2)		

¹2/3-Y,1/3+X-Y,1/3+Z; ²-1/3+Y,1/3-X+Y,4/3-Z; ³1/3-X,2/3-Y,5/3-Z; ⁴1/3-X,2/3-Y,2/3-Z; ⁵2/3-Y,1/3+X-Y,-2/3+Z; ⁶+Y,-X+Y,1-Z; ⁷1/3-Y,2/3+X-Y,-1/3+Z; ⁸1/3+Y-X,2/3-X,-1/3+Z; ⁹1/3+Y-X,2/3-X,2/3+Z; ¹⁰-1/3+Y-X,1/3-X,1/3+Z; ¹¹-Y+X,+X,1-Z.

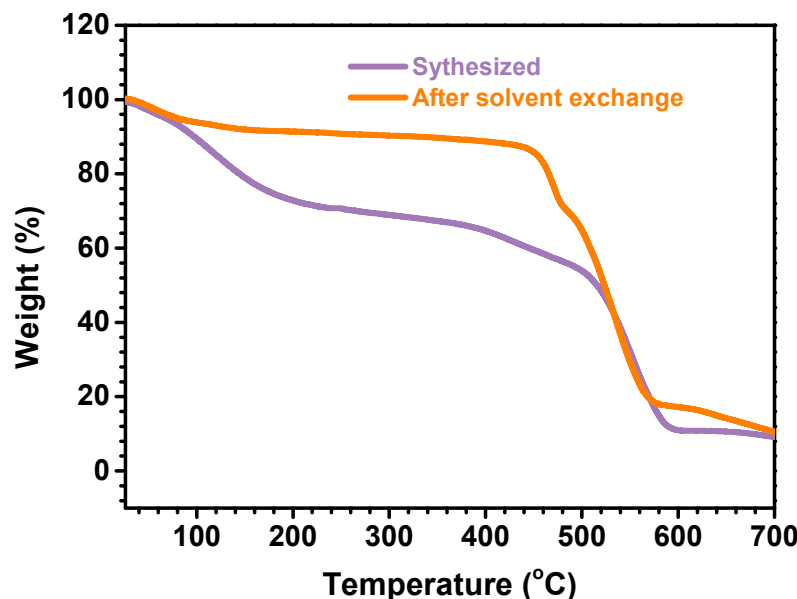


Fig. S2 TGA curves for SNNU-616-Sc.

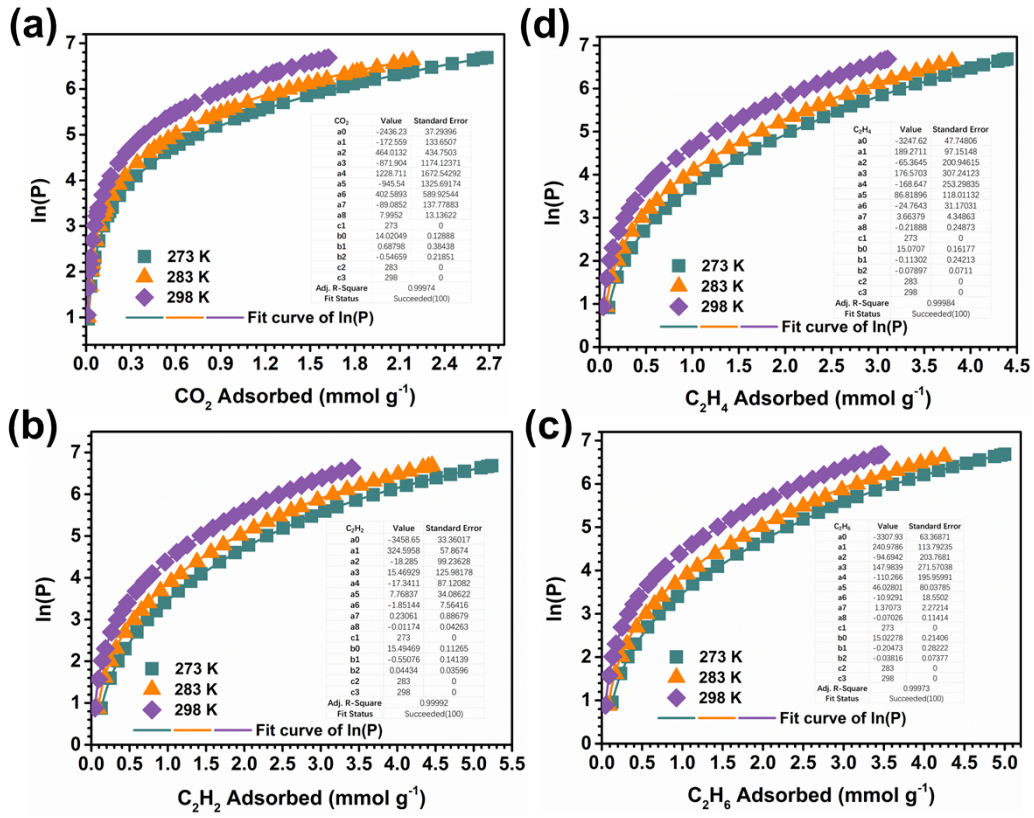


Fig. S3 Virial fitting (lines) of CO_2 , C_2H_4 , C_2H_2 , C_2H_6 (a-d) adsorption isotherms (points) for SNNU-616-Sc at 273, 283, 298 K.

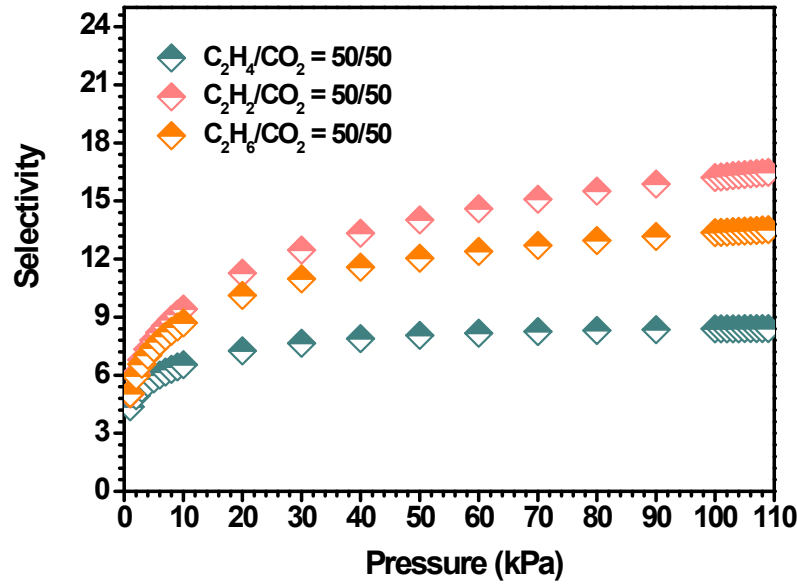


Fig. S4 IAST selective separation ratio for equimolar CO_2 and C_2 -hydrocarbons (C_2H_4 , C_2H_2 , C_2H_6) at 298 K and 1 bar.

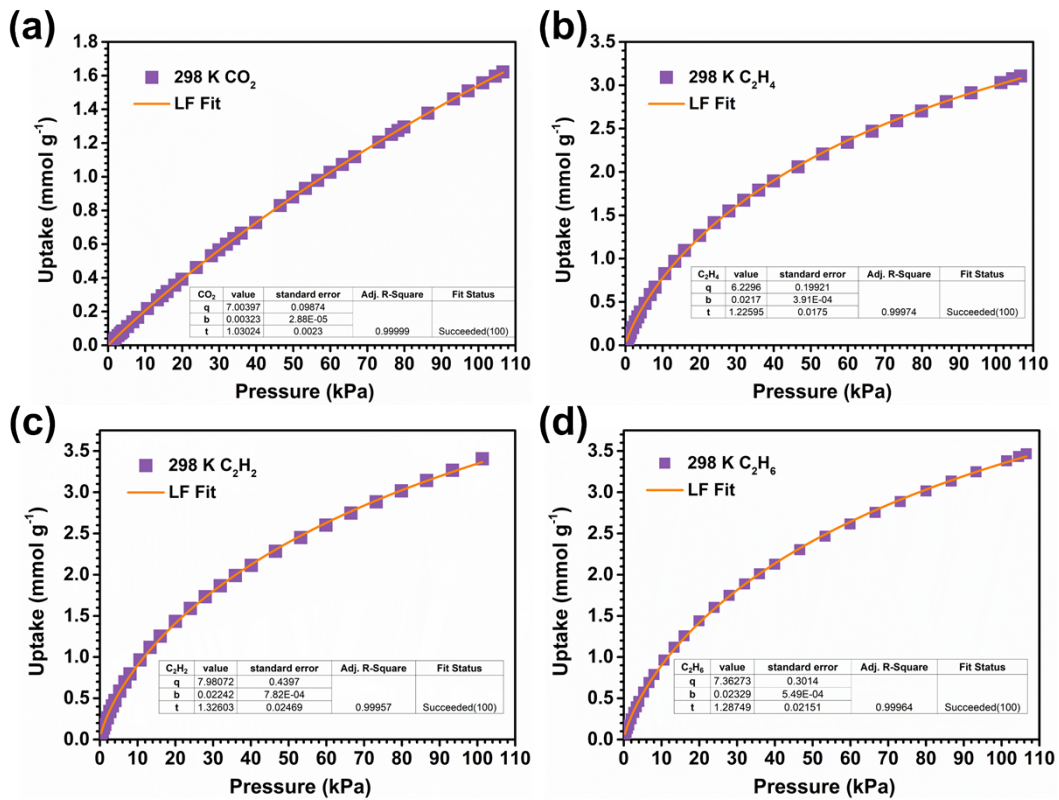


Fig. S5 Langmuir-Freundlich fit curves (lines) to the adsorption data (points) at 298 K for SNNU-616-Sc of CO_2 , C_2H_4 , C_2H_2 , and C_2H_6 (a-d).

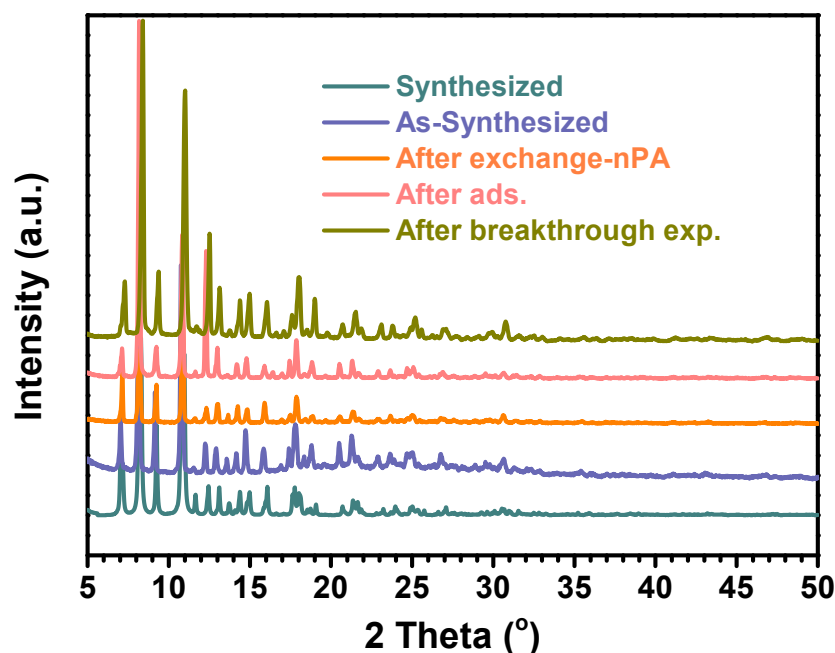


Fig. S6 The PXRD patterns for SNNU-616-Sc after different treatments.

Table S4 High-pressure CO₂ storage data of SNNU-616-Sc at 273 K.

SNNU-616-Sc			
Pressure/bar	Gravimetric uptake/mmol g ⁻¹	Gravimetric Uptake/cm ³ g ⁻¹	wt/%
2.297459751	4.9150	110.0968	13.5228
3.951761021	7.1723	160.6585	18.5792
4.996166641	8.4101	188.3872	21.1090
5.884958141	9.6379	215.8888	23.4674
6.971465635	11.0537	247.6021	26.0178
7.929806645	12.3794	277.2995	28.2566
8.832321965	13.5316	303.1080	30.0950
10.074443565	14.3759	322.0191	31.3834
10.986263165	15.6278	350.0633	33.2089
11.902734905	16.3723	366.7399	34.2491
13.079726535	17.1511	384.1856	35.3031
14.014806845	17.7790	398.2505	36.1286
14.935930725	18.4442	413.1495	36.9804
16.061748805	19.1439	428.8229	37.8523
17.001481245	19.7482	442.3590	38.5861
17.871431585	20.3485	455.8059	39.2981
19.020510365	21.1315	473.3463	40.2024
19.936982105	21.8547	489.5457	41.0140
20.830193145	22.4740	503.4186	41.6917
22.300269645	23.5822	528.2415	42.8662
23.812215415	24.9820	559.5963	44.2838
25.012467745	26.0386	583.2644	45.3082
25.910330925	26.9480	603.6351	46.1602
26.822150525	27.8173	623.1074	46.9501
28.027054995	28.8319	645.8340	47.8432
27.999142155	29.0352	650.3894	48.0187
28.920266035	30.0110	672.2473	48.8442

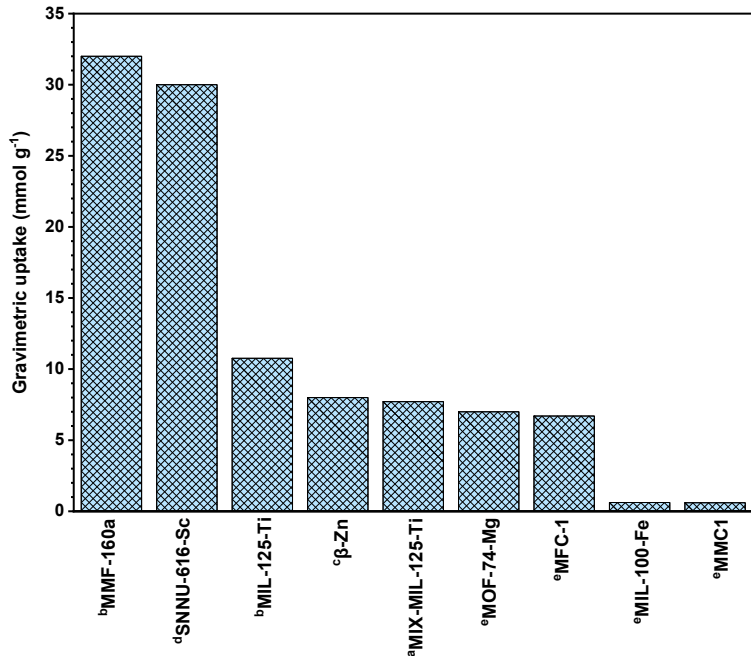


Fig. S7 Comparison of the CO₂ storage capacity of SNNU-616-Sc at 273 K with some reported MOF materials (a-9.8 bar, b-19.8 bar, c-28 bar, d-29 bar, and e-30 bar).

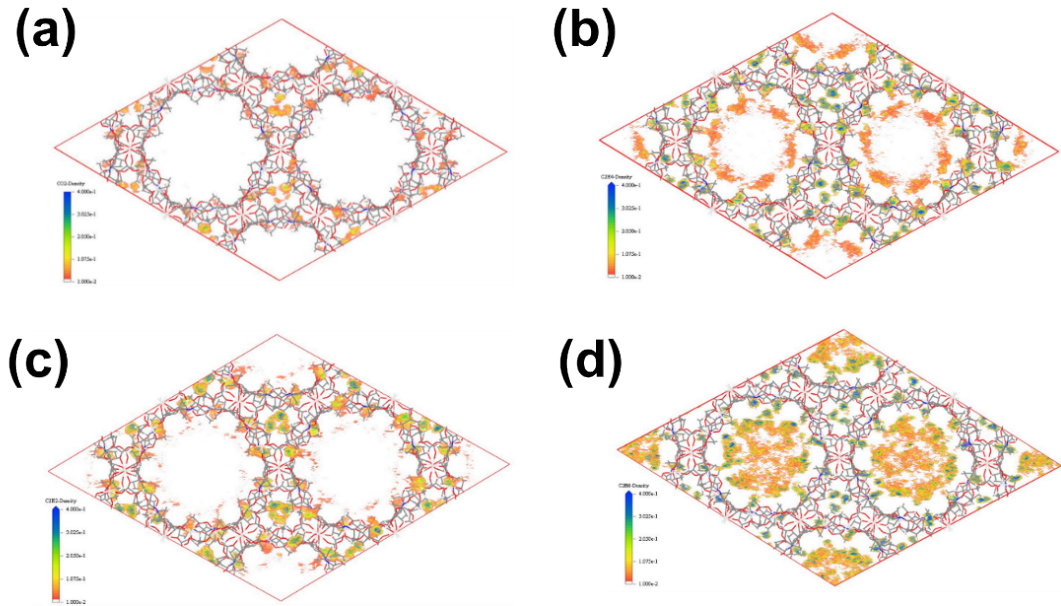


Fig. S8 The GCMC simulated distributions in SNNU-616-Sc for (a) CO₂, (b) C₂H₄, (c) C₂H₂, and (d) C₂H₆.

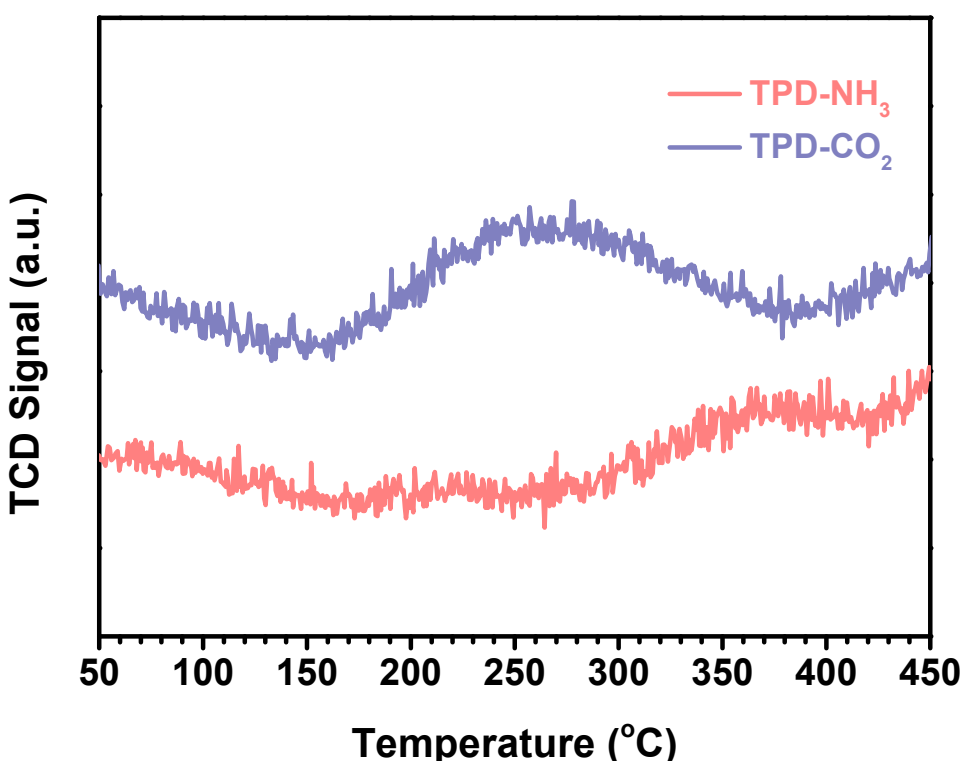


Fig. S9 NH₃-TPD and CO₂-TPD profiles for SNNU-616-Sc catalyst.

REFERENCES

- [S1] Rowsell, J. L. C.; Yaghi, O. M., Effects of Functionalization, Catenation, and Variation of the Metal Oxide and Organic Linking Units on the Low-Pressure Hydrogen Adsorption Properties of Metal-Organic Frameworks. *J. Am. Chem. Soc.* **2006**, *128*, 1304-1315.
- [S2] Bae, Y.-S.; Mulfort, K. L.; Frost, H.; Ryan, P.; Punnathanam, S.; Broadbelt, L. J.; Hupp, J. T.; Snurr, R. Q., Separation of CO₂ from CH₄ Using Mixed-Ligand Metal-Organic Frameworks. *Langmuir* **2008**, *24*, 8592-8598.
- [S3] Gao, J.; Qian, X.; Lin, R.-B.; Krishna, R.; Wu, H.; Zhou, W.; Chen, B., Mixed Metal–Organic Framework with Multiple Binding Sites for Efficient C₂H₂/CO₂ Separation. *Angew. Chem. Int. Ed.* **2020**, *59* (11), 4396-4400.